Pressure dependence of the spin dynamics around a quantum critical point: an inelastic neutron scattering study of $Ce_{0.87}La_{0.13}Ru_2Si_2$

2001 J. Phys.: Condens. Matter 13 8303

(http://iopscience.iop.org/0953-8984/13/36/306)

INSTITUTE OF PHYSICS PUBLISHING JOURNAL OF PHYSICS: CONDENSED MATTER

J. Phys.: Condens. Matter **13** (2001) 8303–8315 PII: S0953-8984(01)22709-X

Pressure dependence of the spin dynamics around a quantum critical point: an inelastic neutron scattering study of $Ce_{0.87}La_{0.13}Ru_2Si_2$

S Raymond[1], **L P Regnault**[1], **J Flouquet**[1], **A Wildes**[2] **and P Lejay**[3]

[1] CEA-Grenoble, DRFMC/SPSMS/MDN, 38054 Grenoble Cédex, France
[2] Institut Laue–Langevin, 38042 Grenoble Cédex, France
[3] CRTBT-CNRS, 38042 Grenoble Cédex, France

Received 7 March 2001, in final form 26 June 2001
Published 23 August 2001
Online at stacks.iop.org/JPhysCM/13/8303

Abstract

Inelastic neutron scattering experiments performed on a single crystal of the antiferromagnetic compound $Ce_{0.87}La_{0.13}Ru_2Si_2$ under applied pressures of up to 5 kbar are reported. A quantum critical point is reached at around 2.6 kbar where long-range magnetic order disappears. The variation of the characteristic energy scales with respect to temperature and pressure is followed and found to saturate in the ordered phase.

1. Introduction

Much experimental and theoretical work has been devoted to the study of quantum phase transitions in recent years [1–4]. Such a transition from an ordered to a disordered state occurs at zero temperature as a function of a control parameter r (pressure P, magnetic field H, impurity concentration x). Heavy-fermion (HF) compounds provide an opportunity to study such phenomena since a variety of ground states, from weak antiferromagnetic to Pauli paramagnetic states, can be realized by tuning r. HF physics has long been understood from the point of view of the so-called Doniach phase diagram describing the competition between the formation of a non-magnetic Kondo singlet and the realization of an ordered state via the RKKY (Ruderman–Kittel–Kasuya–Yosida) interactions [5]. Renewed interest in this field has come about because of accurate studies of the quantum critical point (QCP) in itinerant magnets and the marginal behaviour observed near the QCP, in particular the so-called non-Fermi liquid (NFL) behaviour [1, 4].

Only a few studies have been performed on single crystals using inelastic neutron scattering (INS). The study of a single-crystalline sample on a three-axis spectrometer (TAS) allows the measurement of the full $(\boldsymbol{Q}, \omega)$ dependence of the imaginary part of the dynamical spin susceptibility $\chi''(\boldsymbol{Q}, \omega)$. At present, only two systems have been extensively studied near the QCP: $CeCu_6$ doped with Au at the Cu site [6] and $CeRu_2Si_2$ doped with La at the Ce site [7]. For the latter systems, experiments involving Rh substitution at the Ru site were

also performed [8]. In these works, the magnetic excitation spectra of two samples were studied, one in the paramagnetic phase ($x < x_c$) and one located near the instability point ($x = x_c$). While these two studies produced similar experimental results—reduction of the energy scale near the QCP and increase of the correlation length—the emphasis was put on different points. For $CeCu_{6-x}Au_x$, the anisotropy of the magnetic response [9] was put forward as an explanation of the NFL behaviour observed in bulk measurements, and ω/T scaling was found in the dynamical spin susceptibility [10]. In the latter $Ce_{1-x}La_xRu_2Si_2$ system, the accent was put on the self-consistent renormalized spin-fluctuation (SF) theory of Moriya [3] which allows one to link the magnetic excitation spectrum to the bulk measurements and their evolution towards the QCP [11, 12].

Here we propose a different experimental approach starting from an antiferromagnetic compound and studying the evolution of the magnetic excitation spectrum with pressure up to 5 kbar. This spans the phase diagram through the QCP at finite temperature. The main advantage is that the same crystal is used throughout, avoiding the problem of disorder which is difficult to handle when results obtained on crystals with different concentrations x are compared. The disadvantage is that the temperature range is limited by the experimental set-up (pressure cell) both on the lower- and higher-temperature sides.

2. Experimental details

$CeRu_2Si_2$ crystallizes in the body-centred-tetragonal $I4/mmm$ space group with the lattice parameters $a = b = 4.197$ Å and $c = 9.797$ Å. The dependence of these parameters on the La concentration is roughly linear and of the order of 5×10^{-4} Å/at.% La. The crystal studied here with $x = 0.13$, grown by the Czochralski method, has a volume of 250 mm^3 [13].

Experiments were carried out on the cold TAS IN14 at the ILL high flux reactor, Grenoble. A first set of measurements were performed in a standard orange cryostat at ambient pressure and a second set were carried out in a helium-transmitting-medium pressure cell made of Al alloy in a large-He-flow orange cryostat. The experimental conditions were the same for the two experiments, using the constant-final-energy mode with $k_F = 1.97$ $Å^{-1}$. The collimations were open–40′–60′–60′ and a graphite filter was used in order to reduce higher-order contamination. With this set-up the width of the incoherent peak (full width at half-maximum (FWHM) of a Gaussian profile) was 0.35 meV. These conditions were chosen to minimize the background (flat analyser and collimations), which appears to be crucial for the experiment in the pressure cell. A window of cadmium (neutron absorber) was put around the cryostat in order to reduce the background of the pressure cell. Measurements were performed above 2.6 K to avoid superfluid He from the flow around the pressure cell being present.

3. Determination of the critical pressure

Magnetic ordering occurs in $Ce_{1-x}La_xRu_2Si_2$ for $x \geqslant 0.08$ ($x_c = 0.075$). The ordering takes the form of a sine-wave-modulated structure with the incommensurate wavevector $\boldsymbol{k} = (0.31, 0, 0)$ and the magnetic moments along the c-axis [14]. For the sample studied here ($x = 0.13$), the Néel temperature is $T_N = 4.4$ K with a magnetic moment of 1.05 μ_B at 1.5 K and at ambient pressure. The (P, T) phase diagram of this sample was obtained by studying the evolution of the magnetic Bragg peak $\boldsymbol{Q} = (0.69, 1, 0)$ as a function of pressure ($\boldsymbol{Q} = \tau - \boldsymbol{k}$ where $\tau = (1, 1, 0)$ is a reciprocal-lattice translation). The corresponding neutron peak intensity versus temperature at ambient pressure without the cell and at 1.5 kbar in the pressure cell is shown in figure 1. The pressure variation of the Néel temperature is shown in the inset of figure 1. The

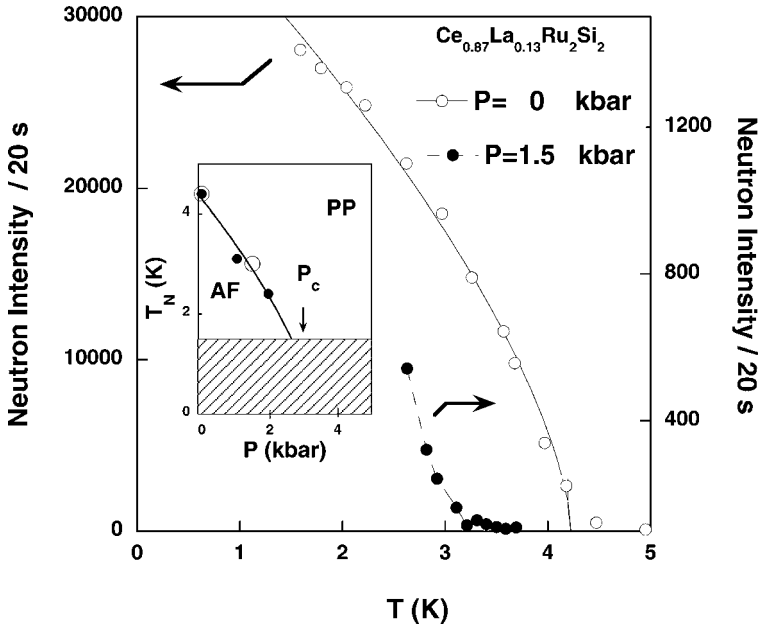

Figure 1. Neutron peak intensity versus temperature measured at $\boldsymbol{Q} = (0.69, 1, 0)$ at $P = 0$ and 1.5 kbar. The lines are guides for the eyes. The inset shows the pressure variation of the Néel temperature. The different symbols correspond to data obtained during two runs of the experiment. The line corresponds to the power-law fit explained in the text. The hatched area corresponds to the temperature range not covered by this experimental set-up.

full-circle data come from a preliminary experiment performed under similar experimental conditions at Laboratoire Léon Brillouin, Saclay, France, while the open-circle ones come from the present study. The agreement between several sets of data indicates the experimental accuracy of the two different series of experiments and shows the reproducibility of the applied pressure. Above 2.8 kbar, no sign of magnetic ordering is found down to 1.8 K. If the pressure variation of the Néel temperature is fitted according to the relation expected for a three-dimensional antiferromagnet near the QCP:

$$T_N \propto (P - P_c)^{2/3} \tag{1}$$

the critical pressure is $P_c = 3.4$ kbar. It is also predicted that the $T = 0$ staggered magnetic moment m_k will follow the relation

$$m_k \propto (P - P_c)^{1/2}. \tag{2}$$

The data shown in figure 1 indicate that the magnetic moment at $0.8T_N$ is reduced by more than one order of magnitude between $P = 0$ and $P = 1.5$ kbar. In view of this observation, even if we lack very low-temperature data, m_k will certainly not follow a simple law like (2). Such a deviation from the theoretical prediction (2) was studied in detail for alloys of the family $Ce(Ru_{1-x}Rh_x)_2Si_2$ [15, 16]. (This is not the purpose of the present work, which concentrates on the dynamics.) It is thus difficult to extract P_c from the pressure variation of m_k; an upper estimate would be 2.2 kbar. Another estimate of P_c can be derived from the bulk measurements performed on several concentrations or under pressure in this family of compounds. Resistivity measurements performed for $x = 0.2$ under pressure show that 2.4% of lanthanum substitution corresponds to 1 kbar [17]. For the compound studied here with

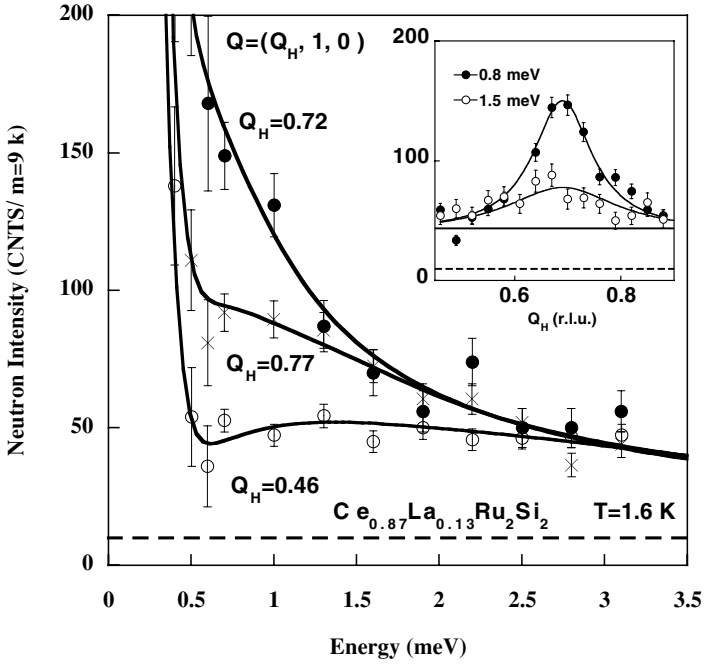

Figure 2. Constant-$\boldsymbol{Q}$ scans realized at 2.6 K and $P = 0$ kbar around the wavevector of the instability $\boldsymbol{k}$. Lines correspond to the fit explained in the text. The inset shows two constant-energy scans performed at 0.8 and 1.5 meV. The dashed line indicates the background of the spectrometer. The solid straight line in the inset corresponds to the single-site contribution.

$x = 0.13$, this will give an expected P_c of 2.1 kbar. In the following, we will take the mean value of these three different estimates: $P_c = 2.6 \pm 0.5$ kbar.

4. The magnetic excitation spectrum at $P = 0$

$CeRu_2Si_2$ has a strong Ising character [18] and exhibits only longitudinal fluctuations (fluctuations of the order parameter) as established by INS [19]. Therefore INS experiments are carried out in the basal plane of the tetragonal structure since neutron scattering probes fluctuations perpendicular to the scattering vector $\boldsymbol{Q}$. The magnetic excitation spectrum is shown in figure 2 for several $\boldsymbol{Q}$-vectors ($\boldsymbol{Q} = (Q_H, 1, 0)$ where Q_H is expressed in reciprocal-lattice units (r.l.u.)) at 2.6 K. The corresponding wavevector response is shown in the inset of figure 2 for two energy transfers of 0.8 and 1.5 meV. The signal is peaked at $Q_H = 0.69$ for both energies and the lineshape broadens when energy increases. The response in energy is quasielastic as shown in figure 2 for $Q_H = 0.72$. This wavevector is chosen to be $\boldsymbol{k} + (0.03, 0, 0)$ where $\boldsymbol{k}$ is the wavevector of the instability, in order to avoid strong Bragg contamination. This offset has no consequences for the physical quantities determined (energy widths), since the signal that we measured does not vary rapidly around $\boldsymbol{k}$ in the energy range probed with our instrumental resolution. Despite the fact that the compound is ordered, the spectrum is characteristic of SF and no well-defined (single-mode) excitations are observed. The background of the spectrometer (determined for negative energy transfer at low temperature) does not correspond to the background of the constant-ω scan, suggesting the existence of a $\boldsymbol{Q}$-independent (or single-site) contribution as in other compounds of this family [11, 21, 22].

Consequently, we used the same procedure as in the previous works on $x = 0$ [22] and $x_c = 0.075$ [11] compounds to carry out a quantitative analysis of the data. This procedure accounts for the background in a consistent way for both constant-$\boldsymbol{Q}$ and constant-ω scans. In the first works on $CeRu_2Si_2$, the single-site contribution was not taken into account [20] since only high-magnetic-field studies unambiguously indicate the existence of this contribution [21, 22]. On applying a magnetic field, the correlated part of the signal vanishes and only the $\boldsymbol{Q}$-independent contribution persists at the same level of intensity as was determined at $H = 0$. In a similar fashion to in the applied external magnetic field case, we will also show that this decomposition of the magnetic scattering into single-site and correlated signals is very convenient for understanding experiments carried out under pressure. In this approach, the neutron intensity is written as follows:

$$I(\boldsymbol{Q}, \omega) = I_{BG} + (1 + n_B(\omega))(\chi''_{SS}(\omega) + \chi''_{IS}(\boldsymbol{Q}, \omega)) \tag{3}$$

where $\boldsymbol{I}_{BG}$ is the background intensity, $n_B(\omega) = 1/(e^{\omega/T} - 1)$ is the Bose factor and χ''_{SS} and χ''_{IS} are respectively the imaginary parts of the single-site and intersite magnetic dynamical susceptibility. The single-site contribution is assumed to be Lorentzian, reflecting local 4f spin relaxation:

$$\chi''_{SS}(\omega) = \chi'_{SS}\frac{\omega\Gamma_{SS}}{\omega^2 + \Gamma^2_{SS}} \tag{4}$$

where χ'_{SS} is the local susceptibility and Γ_{SS} is the local fluctuation rate. It is related to the Kondo temperature T_K ($\Gamma_{SS} \approx k_B T_K$ [23]). For the correlated signal, we use the following formula, where $\boldsymbol{q} = \boldsymbol{Q} - \boldsymbol{\tau} - \boldsymbol{k}$:

$$\chi''_{IS}(\boldsymbol{q}, \omega) = \frac{\chi'_{IS}(\boldsymbol{q})}{2}\omega\left(\frac{\Gamma_{IS}(\boldsymbol{q})}{(\omega - \omega_0(\boldsymbol{q}))^2 + \Gamma^2_{IS}(\boldsymbol{q})} + \frac{\Gamma_{IS}(\boldsymbol{q})}{(\omega + \omega_0(\boldsymbol{q}))^2 + \Gamma^2_{IS}(\boldsymbol{q})}\right) \tag{5}$$

where $\chi'_{IS}(\boldsymbol{q})$ is the $\boldsymbol{q}$-dependent part of the susceptibility, $\Gamma_{IS}(\boldsymbol{q})$ is the intersite fluctuation rate and $\omega_0(\boldsymbol{q})$ is an inelastic energy which clearly describes better the data obtained for compounds of this family located in the paramagnetic region [22]. In this paper, we will focus on the response in energy at the wavevector $\boldsymbol{k}$ and will note that $\Gamma_{IS} = \Gamma_{IS}(q = 0)$. It is also found that $\omega_0(\boldsymbol{q})$ does not depend on $\boldsymbol{q}$, as was already known from studies of other compositions.

The single-site contribution is determined at $\boldsymbol{Q} = (0.46, 1, 0)$ in a part of the Brillouin zone where the signal is flat in $\boldsymbol{q}$ (see the inset of figure 2) and thus $\chi'_{IS} = 0$. The fit to the data is shown in figure 2. Since the neutron intensity is not normalized, we are only interested in the energy width, $\Gamma_{SS} = 1.4(2)$ meV. A fit at the vector $\boldsymbol{k}$ is also shown in figure 2. We found for the offset $q_H = 0.03$ ($\boldsymbol{q} = (q_H, q_K, q_L)$) at 2.6 K in the ordered phase the values $\Gamma_{IS} = 0.15(3)$ meV and $\omega_0 = 0.10(5)$ meV. Contrary to the case for the pure compound $CeRu_2Si_2$, the determination of ω_0 lies at the limits of the fit since it is smaller than the resolution. It is worth noting that the value of Γ_{IS} determined does not change much if ω_0 is fixed at zero. For comparison, the values obtained at 2.6 K for the compounds corresponding to $x = 0$ and $x_c = 0.075$ are shown in table 1. The q_H-dependence was described by expanding $\Gamma_{IS}(q_H) = \Gamma_{IS}(1+ (q_H/\kappa)^2)$ in (5) and assuming that $\chi_{IS}(q_H)\Gamma_{IS}(q_H) =$ constant [24]. The fits to the data obtained at 0.8 and 1.5 meV are shown in the inset of figure 2 with a value of $\kappa = 0.05$ r.l.u. This corresponds to a correlation length $\xi \approx 13$ Å that is around three lattice units. This is the correlation length of the remaining fluctuations after magnetic order is established in this system. This must not be confused with the correlation length introduced in phase transition theory which diverges at T_N or at P_c. This latter quantity needs to be measured in a double-axis configuration in order to obtain an energy-integrated signal.

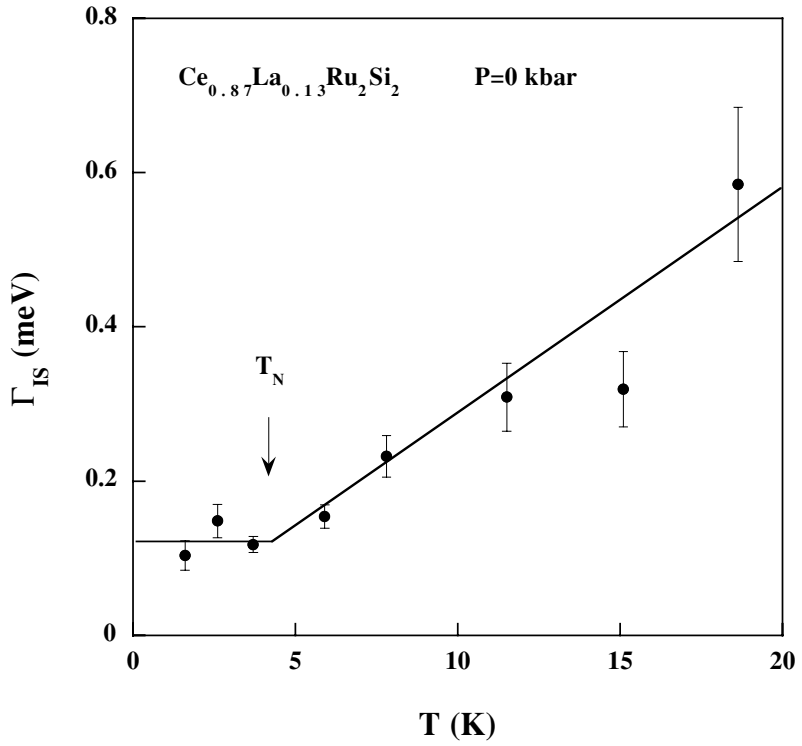

Figure 3. The temperature dependence of the fluctuation rate Γ_{IS} measured at $P = 0$ kbar. The line is a guide for the eyes.

Table 1. Characteristic energies (in meV) measured at 2.6 K for several compounds of the family $Ce_{1-x}La_xRu_2Si_2$ for $\boldsymbol{Q} = \boldsymbol{k}$ under similar experimental conditions (cold TAS).

x	Γ_{IS}	ω_0	Γ_{SS}
0	0.77(5)	0.5(1)	2.0(1)
0.075	0.17(2)	0.2(1)	1.4(1)
0.13	0.15(3)	0.10(5)	1.4(2)

The analysis was repeated for several temperatures. On increasing T, the magnetic excitation spectrum broadens continuously. Of interest is the temperature variation of Γ_{IS}. This quantity is shown in figure 3. The temperature variation is almost linear above T_N, slowing down and eventually saturating below T_N. In contrast, the quantity Γ_{SS} is almost temperature independent in the range studied, 1.5–20 K. At higher temperature, for $\Gamma_{SS} > k_B T$, it is expected that Γ_{SS} will acquire some temperature dependence [23].

5. Evolution of the magnetic excitation spectrum with pressure

Like the temperature dependence studied at zero pressure, we also studied the evolution of the spin dynamics with pressure at a constant temperature of 2.6 K. Figure 4 shows the neutron intensity measured versus pressure for two energy transfers of 1 and 6 meV. The spectrometer background measured for an energy transfer of -1 meV at 2.6 K is subtracted. Although it

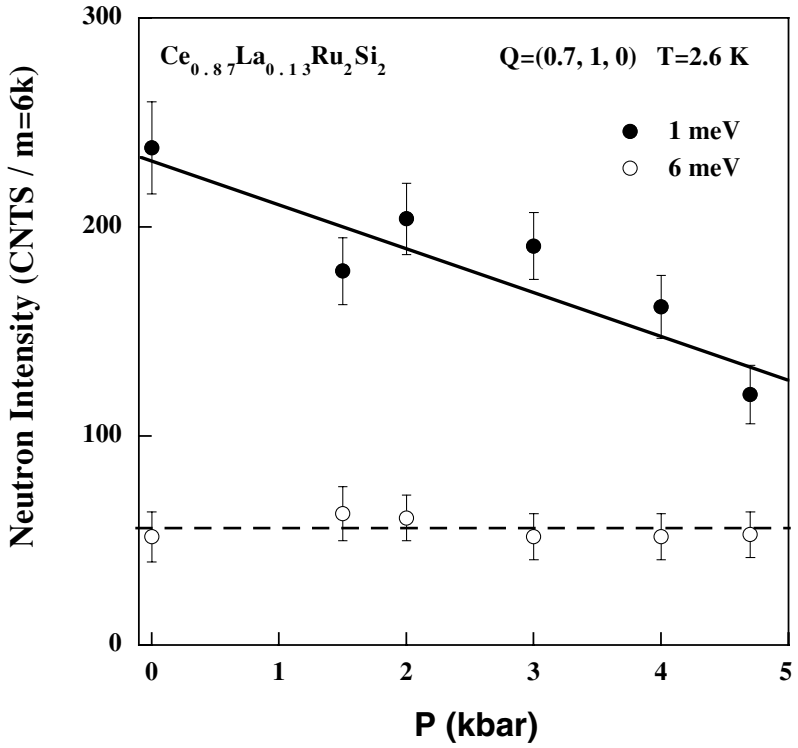

Figure 4. The pressure dependence of the inelastic magnetic scattering measured at $\boldsymbol{Q} = (0.7, 1, 0)$ for 1 meV (full circles) and 6 meV (open circles) energy transfer at 2.6 K. The spectrometer background is subtracted. Lines are guides for the eyes.

is difficult to interpret such data (changes in intensity can originate from changes either in the susceptibility or in the linewidth), there is clearly a difference in behaviour between the low- and high-energy data. The former energy response decreases when pressure increases while the latter one is not sensitive to pressure. A crossover between low-energy and high-energy dynamics therefore needs to be defined. In the framework of the quantum phase transition and for a gapless system [4], this crossover energy Δ is the relevant quantity for studying the QCP (i.e. $\Delta \to 0$ at the QCP). The analysis of the dynamical spin susceptibility of this system as single-site and intersite contributions provides us with a natural way of defining such a crossover. Indeed, the high-energy part corresponds to a single-site-only contribution. In the following, we will simply take $\Delta \approx \Gamma_{IS}$. In this respect, pressure and magnetic field suppress the intersite contribution in similar ways (see figure 8 of reference [22] in comparison with figure 4).

Figure 5 shows the evolution of the intersite signal measured at $\boldsymbol{Q} = (0.7, 1, 0)$ after subtraction of the data from the single-site signal measured at each pressure at $\boldsymbol{Q} = (0.46, 1, 0)$. At zero pressure (upper frame), a Bragg contribution appears. The spectrometer configuration is chosen such that, with the offset $q_H = 0.01$, the resolution ellipsoid catches the Bragg peak tail at negative energy transfer. The inelastic signal broadens with increasing pressure and at 4.7 kbar it is very similar to that of the pure compound $CeRu_2Si_2$ (see figure 9 in reference [22]).

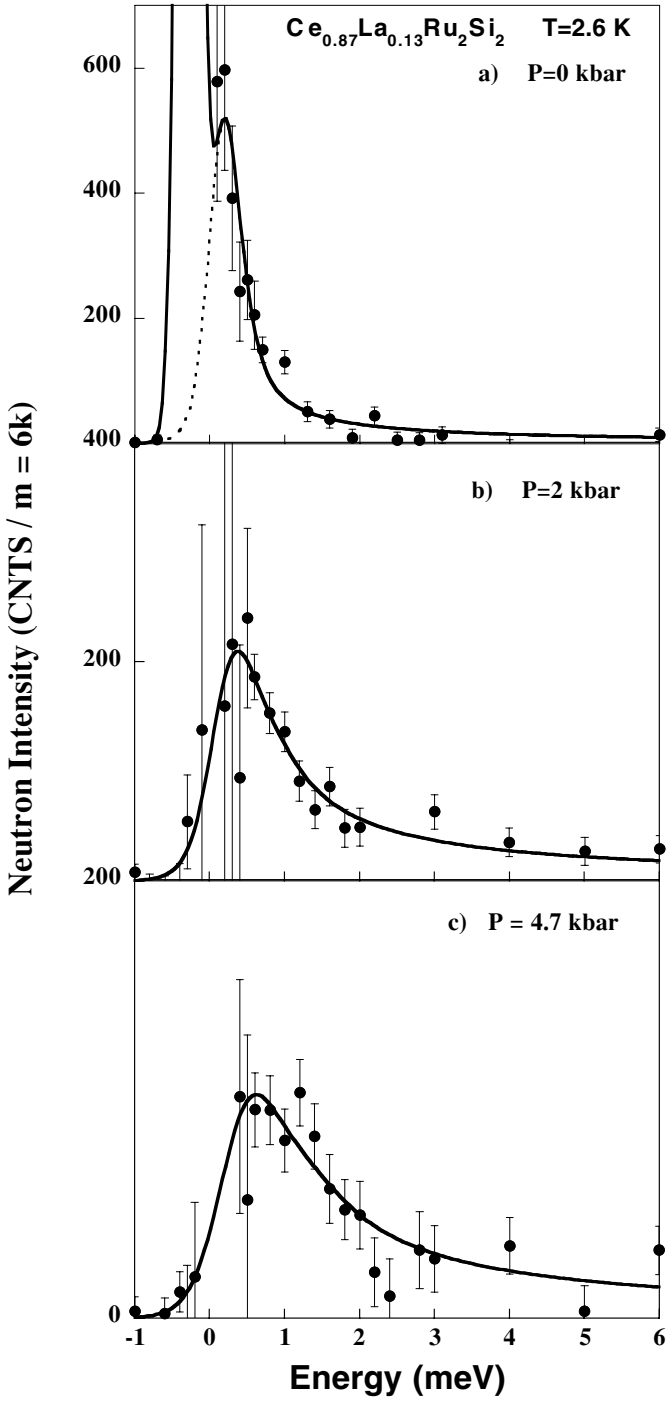

Figure 5. The evolution with pressure of the intersite contribution of the dynamical spin susceptibility measured at 2.6 K at 0, 2 and 4.7 kbar. The experimental data are obtained by point-by-point subtraction of $\boldsymbol{Q} = (0.7, 1, 0)$ to $\boldsymbol{Q} = (0.46, 1, 0)$.

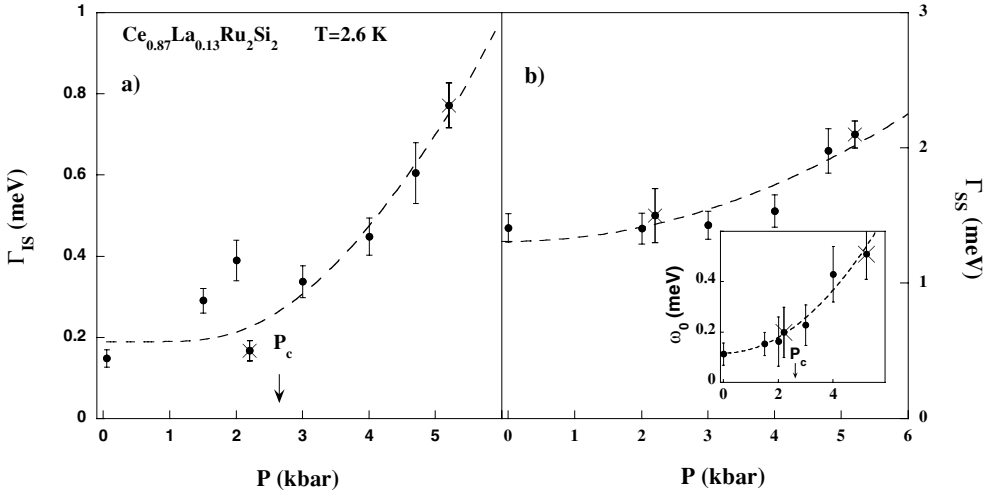

Figure 6. (a) The pressure dependence of the fluctuation rate Γ_{IS} measured at 2.6 K. (b) The pressure dependence of the local fluctuation rate Γ_{SS} measured at 2.6 K. The inset shows the pressure dependence of ω_0. For each panel, the crossed circles correspond to data obtained for the alloys with $x = 0$ and $x_c = 0.075$ with the pressure–concentration conversion explained in the text. Lines correspond to the fit explained in the text.

The pressure variation of Γ_{IS} is shown in figure 6(a). The data obtained at the same temperature for the alloy corresponding to the critical concentration, $x_c = 0.075$, and to the pure compound, $x = 0$, are shown in the same plot with the pressure–concentration conversion taken from resistivity measurements as mentioned in the first section and leading to $P = 5.2-0.4x$ with x in %. There is a reasonably good agreement between these former measurements and our present measurements under pressure. The data presented in this way exhibit some noise due to the fact that they were taken from different experiments with different set-ups. There is thus no correlation between the error bars for the points obtained under pressure and those for the ones obtained for the alloys. Furthermore, the data taken under pressure lead also to higher error bars since the background is higher. Nevertheless, this agreement emphasizes the validity of the analogy between concentration and pressure in the limit of small disorder.

Despite the limited statistics of the data, it seems that the energy width as a function of pressure saturates below the critical pressure P_c similarly to its saturation as a function of temperature below T_N at $P = 0$. Indeed the two sets of data, $\Gamma_{IS}(P)$ and $\Gamma_{IS}(T)$, are strikingly similar. The data clearly show that the increase of Γ_{IS} is much higher in the non-magnetic phase above 3 kbar. To reproduce this behaviour, we made a global fit of these data to the phenomenological expression

$$\Gamma_{IS}(P) = \Gamma_{IS}(0) + \alpha P \exp(-P^*/P) \tag{6}$$

with $\Gamma_{IS}(0) = 0.19(2)$ meV, $\alpha = 0.4(2)$ meV kbar^{-1} and $P^* = 7(2)$ kbar. This expression reproduces the saturation of Γ_{IS} at low pressure and is linear in P for $P \gg P^*$. The pressure variation of Γ_{SS} is shown in figure 6(b). This quantity increases only slightly in the pressure range studied. This confirms the idea that the high-energy dynamics does not change much with pressure. The data are phenomenologically described by the smooth variation $\Gamma_{SS} = \Gamma_{SS}(0) + \eta P^2$ with $\Gamma_{SS}(0) = 1.3(1)$ meV and $\eta = 0.025(5)$ meV kbar^{-2}. Finally, the pressure variation of ω_0 is shown in the inset of figure 6(b). It is very similar to that of Γ_{IS}. The relation $\omega_0 \propto 0.6\,\Gamma_{IS}$ holds approximately. Beyond these phenomenological descriptions, an

order of magnitude can be extracted for the pressure variation of the different characteristic energies ϵ ($\epsilon = \Gamma_{IS}$, Γ_{SS} or ω_0). Taking the pressure range studied (ΔP) as a whole, all these quantities increase with quite similar rates of $\Delta\epsilon/\Delta P \approx 1$ K kbar^{-1}.

6. Discussion

6.1. Nature of the excitations

We first discuss the nature of the excitations in the ordered phase. Due to the strong Ising nature of the system, the observation of spin waves by means of INS is precluded. The fact that the excitations are not well-defined dispersive modes is understood from the magnetic structure of the system. For an incommensurate structure, $\boldsymbol{q}$ is not a good quantum number due to the lack of translational invariance. INS measurements probe the dynamical susceptibility at ($\boldsymbol{q}$, ω) and this corresponds here to the coupling of several eigenmodes giving a broad signal [25]. This is not the case for real antiferromagnetic structure, where longitudinal well-defined dispersive modes can be observed in compounds with weak magnetic moments. Such modes were measured by means of INS in URu_2Si_2 [26].

Our data show similar results when the ordered phase is reached either by varying temperature or pressure. The fluctuation rate seems to reach a constant and finite value in the ordered phase. This behaviour can be partly understood from the point of view of the magnetic sum rule which states that the total magnetic scattering integrated over $\boldsymbol{q}$ and ω is proportional to the square of the magnetic moment of the ion (in fact $S(S+1)$ in the quantum mechanical treatment of a spin S). Since the ordered moment at $T \approx 0$, $P \approx 0$($m_k = 1.05\,\mu_B$) does not reach the saturated value (m_{sat}) determined by the crystal-field ground state ($\approx$1.7 μ_B), and since spin waves are not present, the presence of longitudinal fluctuations is necessary in order to satisfy the magnetic sum rule. In particular, we do not observe any complete softening either of Γ_{IS} (P) at P_c or of Γ_{IS} (T) at T_N. This can also be partly understood on the basis of the same argument. This is also linked to the itinerant nature of the magnetic order, as discussed in the following subsection.

6.2. Analysis in a spin-fluctuation approach

Our data suggest that the magnetic order has the form of a spin-density wave at least down to the lowest measured temperature of 1.5 K. Firstly, we are able to accurately follow the local fluctuation rate, Γ_{SS}, as a function of pressure, which does not vanish at the QCP but smoothly decreases from the disordered to the ordered state. This quantity reflects the mechanism of local relaxation of 4f moments that is the Kondo effect. This implies that there is no breakdown of the Kondo effect at P_c in the $Ce_{1-x}La_xRu_2Si_2$ system. Secondly, the magnetic order realized for $x = 0.13$ is purely sinusoidal since the higher-order harmonics were found with negligible intensity down to the lowest temperatures [27]. This also points towards a SDW picture since such a pure sinusoidal modulation is typical of itinerant magnetism while squaring of the modulation occurs in localized spin systems. Indeed, in $Ce_{1-x}La_xRu_2Si_2$, higher harmonics were found to develop for $x \geqslant 0.2$ [28]. Such a crossover from a SDW to a local magnetism is also observed in the similar $Ce(Ru_{1-x}Rh_x)_2Si_2$ compounds [29]. The underlying hypothesis of an itinerant-magnetism description is that a Fermi surface is well defined throughout the whole phase diagram.

In the past few years, neutron scattering data and bulk measurements obtained on the $Ce_{1-x}La_xRu_2Si_2$ system were self-consistently analysed within Moriya's SF theory [11, 12]. The finite fluctuation rate measured by means of neutron scattering around P_c must obviously

be related to the observation that the resistivity always reaches a T^2-dependence at the lowest temperature and that, concomitantly, the specific heat is always linear in T. Our new INS data confirm such a picture. The dynamical spin susceptibility, which is a phenomenological starting point of SF theory, was also recently deduced form a microscopic model taking the Kondo effect and the RKKY interactions equally into account; the INS cross section derived is very similar to the one used in this paper [30, 31].

6.3. Comparison with $CeCu_{6-x}Au_x$

In the $CeCu_{6-x}Au_x$ system, the QCP is reached for $x \approx 0.1$. NFL behaviour observed either at P_c or x_c in this system (linear resistivity, logarithmic divergence of the specific heat) was extensively studied by the Karlsruhe group [6]. It is believed that such a behaviour implies that a new theoretical treatment of the QCP is required in a strong-coupling approach, a local picture where the Fermi liquid description breaks down [32]. The underlying idea is that both T_N and T_K go to zero at the QCP: the ordered phase is characteristic of local magnetism. For INS, the hallmark of such a behaviour is the so-called ω/T scaling of the dynamical spin susceptibility [10]. In the description developed here, this means that Γ_{IS} equals $k_B T$ (no single-site signal was identified in these studies [9, 10]). This obviously implies that (i) the fluctuation rate totally softens at the QCP[1] and (ii) ω and T are similarly weighted in the spin dynamics. In contrast, in the SF approach, the fluctuation rate Γ_{IS} is written as $y_0 + a' T^{3/2}$ [4, 31, 34] where $y_0 \to 0$ at the QCP and a' is constant. Following this argument, $\omega/T^{3/2}$ scaling would be expected for a three-dimensional system near the QCP (in the case where $a' \approx 1$). This difference from the observed ω/T scaling in $CeCu_{5.9}Au_{0.1}$ has a deeper meaning. In the itinerant-magnetism model [2], a system in the vicinity of a QCP is above the critical dimension ($d_c = 4$, above which the Landau theory is valid). This is linked to the increasing importance of the fluctuations in time at $T = 0$ near the QCP. Formally, this is described by the dynamical exponent z ($z = 2$ for an itinerant antiferromagnet), and the effective dimension of the system becomes $d_{eff} = d + z$ where d is the geometrical dimension [2, 4]. In contrast, the scaling observed in $CeCu_{5.9}Au_{0.1}$ implies that the system is below the critical dimension. The origin of this behaviour is believed to lie in the anomalous spin dynamics [10], implying that the effective dimension is lower by $1/2$ compared to that of the usual scenario of quantum phase transitions. These results need a new theoretical treatment beyond the current understanding of the QCP.

In $Ce_{1-x}La_xRu_2Si_2$, a complete softening of Γ_{IS} is not observed at the QCP as already discussed. For this system, it is experimentally clear that $T_N \to 0$ at the QCP but that T_K stays finite in the ordered phase. This latter quantity may collapse far into the magnetic phase. As regards the temperature variation of Γ_{IS}, it follows the SF prediction ($\Gamma_{IS} = y_0 + a' T^{3/2}$) with $a' \approx 0.2$ meV $K^{-3/2}$ as measured for $x = x_c$. It is important to note that the value of a' is the same for $CeRu_2Si_2$ and thus does not evolve with P or $_x$. The same remark holds for the system $CeCu_{6-x}Au_x$: the slope of the order of unity found *de facto* in the ω/T scaling for Γ_{IS} is also found for pure $CeCu_6$ [33].

The results obtained on the systems $CeCu_{6-x}Au_x$ and $Ce_{1-x}La_xRu_2Si_2$ are quite different since the former seems to be the paradigm of the strong-coupling theory while the latter is the paradigm of SF theory. The behaviour observed at a magnetic–non-magnetic QCP is thus not universal. What still remains surprising is that pure $CeCu_6$ and $CeRu_2Si_2$ compounds are very

[1] This point is difficult to address experimentally by means of INS not only because of the limited access to the lowest temperatures, but also because of the instrumental resolution, which will limit the distinction between statics and dynamics below a certain energy ω.

similar while their respective QCP are so different. As regards the low-energy scales involved for $CeCu_6$, the possibility cannot be excluded that the physics observed corresponds to the fact that the Fermi surface is not yet developed at the temperatures achievable experimentally. To test this possibility, ω/T scaling must be searched for in $Ce_{1-x}La_xRu_2Si_2$ for $k_BT \gg \Gamma_{SS}$ near the QCP. The idea is that such a scaling may apply in a temperature range above the $T^{3/2}$-regime experimentally observed and predicted by SF theory.

7. Conclusions

This study is, to our knowledge, the first INS investigation of the QCP performed on a single crystal where pressure is the control parameter for the magnetic–non-magnetic phase diagram. The data obtained show a quantitative similarity between the approach of the magnetic phase versus pressure or temperature. Our results are in agreement with those from previous experiments performed on alloys near the QCP ($x \approx x_c$) and in the paramagnetic phase $x > x_c$. Our overall data on the compounds of the $Ce_{1-x}Lax Ru_2Si_2$ family strongly support the SF approach. In the future, we will concentrate our efforts on the low-temperature data at P_c and x_c with a view to confirming this picture.

Acknowledgments

We acknowledge the help of J M Mignot with preliminary experiments performed at LLB, Saclay. This work benefited from useful discussions on quantum critical points with C Pépin, M Lavagna, P Haen, K Ishida, K Miyake, S Kambe, B Fåk and N Bernhoeft.

References

[1] See, e.g., *Proc. Int. Conf. on Strongly Correlated Electron Systems* 2000 *Physica* B **281+282**
[2] Millis A 1993 *Phys. Rev.* B **48** 7183
[3] Moriya T and Takimoto T 1995 *J. Phys. Soc. Japan* **64** 960
[4] Sachdev S 1999 *Quantum Phase Transitions* (Cambridge: Cambridge University Press)
[5] Doniach S 1977 *Physica* B **91** 231
[6] von Löhneysen H 2000 *J. Magn. Magn. Mater.* **200** 532
[7] Raymond S *et al* 1999 *Physica* B **259–261** 48
[8] Tabata S *et al* 1999 *Physica* B **259–261** 70
[9] Stockert O *et al* 1998 *Phys. Rev. Lett.* **80** 5627
[10] Schröder A *et al* 1998 *Phys. Rev. Lett.* **80** 5623
[11] Raymond S *et al* 1997 *J. Low Temp. Phys.* **109** 205
[12] Kambe S *et al* 1996 *J. Phys. Soc. Japan* **65** 3294
[13] Lejay P *et al* 1993 *J. Cryst. Growth* **130** 238
[14] Quézel S *et al* 1988 *J. Magn. Magn. Mater.* **76+77** 403
[15] Kawarasaki S *et al* 2000 *J. Phys. Soc. Japan Suppl.* A **69** 53
[16] Kawarasaki S *et al* 2000 *Phys. Rev.* B **61** 4167
[17] Haen P *et al* 1996 *J. Phys. Soc. Japan Suppl.* B **65** 27
[18] Haen P *et al* 1987 *J. Low Temp. Phys.* **67** 391
[19] Jacoud J L 1991 *PhD Thesis* University of Grenoble
[20] Regnault L P *et al* 1988 *Phys. Rev.* B **38** 4481
[21] Jaccoud J L *et al* 1989 *Physica* B **156+157** 818
[22] Rossat-Mignod J *et al* 1988 *J. Magn. Magn. Mater.* **76+77** 376
[23] Kuramoto Y and Kitaoka Y 2000 *Dynamics of Heavy Electrons* (Oxford: Clarendon) pp 81–3
[24] Kuramoto Y 1987 *Solid State Commun.* **63** 467
[25] See, e.g., Ziman T and Lindgård P A 1986 *Phys. Rev.* B **33** 1976
[26] Broholm C *et al* 1991 *Phys. Rev.* B **43** 12809
[27] Raymond S 2001 in preparation

[28] Mignot J M *et al* 1991 *Physica* B **171** 357
[29] Miyako Y *et al* 1997 *Physica* B **230–232** 1011
[30] Pépin C and Lavagna M 1999 *Phys. Rev.* B **59** 2591
[31] Lavagna M and Pépin C 2000 *Phys. Rev.* B **62** 6450
Lavagna M and Pépin C 2001 *Phys. Rev.* B **63** 029901 (erratum)
[32] Coleman P 1999 *Physica* B **259–261** 353
[33] Stockert O 2000 private communication
[34] Hatatani M*et al* 1998 *J. Phys. Soc. Japan* **67** 4002